ELSEVIER

Journal of Structural Geology 27 (2005) 397–408

JOURNAL OF STRUCTURAL GEOLOGY

www.elsevier.com/locate/jsg

What controls relay ramps and transfer faults within rift zones? Insights from analogue models

V. Acocella*, P. Morvillo, R. Funiciello

Dip. Scienze Geologiche Università Roma Tre. Largo S.L. Murialdo, 1, 00146, Rome, Italy

Received 7 May 2004; accepted 8 November 2004
Available online 25 January 2005

Abstract

Structures within rift zones exhibit two main types of interaction relevant at the rift scale: relay ramps and transfer faults at high angle to the rift. Analogue experiments have been performed to investigate whether these types of interaction may be affected by differential extension along the rift. In these models, sand (brittle crust analogue) overlies two adjacent silicone (ductile crust analogue) layers with different viscosity, in order to simulate different percentage extension rates (Δe) along rifts. The experiments show a distinct behaviour as a function of Δe. For $\Delta e < 21 \pm 3\%$, extensional structures interact forming relay ramps; for $\Delta e > 21 \pm 3\%$, the interaction occurs by means of transfer faults striking subparallel to the extension direction. Experimental data are consistent with the geometries and extension rates of rift zones. Relay ramps characterize narrow rifts and oceanic ridges, where the mean percentage of extension is low ($e < 16\%$). Conversely, transfer faults are usually found in extensional settings (passive margins, wide rifts, back-arc basins) with significant stretching ($e > 39\%$), where the rift more likely achieves differential extension $\Delta e > 21\%$.

Keywords: Rift zones; Relay ramps; Transfer faults; Analogue models; Differential extension

1. Introduction

Rift zones are commonly segmented at various scales Segments are, however, transient features in the evolution of a rift zone, as they grow and interact and may link to form larger structures (Macdonald and Fox, 1983; Pollard and Aydin, 1988; Dawers and Anders, 1995; Koukouvelas et al., 1999). Therefore, the process of interaction is a necessary step in the evolution of a rift zone over a range of scales.

Two main typologies of interaction between segments (or groups of segments) that appear to be significant at the scale of the considered rift (controlling its shape or continuity) can be identified. The interaction may develop relay ramps or accommodation zones, which consist of broad areas of ductile strain between extensional structures (grabens, normal faults, extensional fractures) usually characterized by arcuate geometries (Fig. 1; e.g. Peacock et al., 2000a, and references therein). This type of interaction constitutes a common type of 'soft linkage' (Walsh and Watterson, 1991). Conversely, the interaction may develop a transfer fault, which is a subvertical transtensive fault that strikes at high angle and transfers displacement between two adjacent crustal sectors undergoing differential extension (Fig. 1; Gibbs, 1990; Peacock et al., 2000a, and references therein). This type of interaction constitutes a common type of 'hard linkage' (Walsh and Watterson, 1991).

Both types of interaction are found in rift zones. Relay ramps are widespread; they have been described for example in the Rhine Graben (Illies, 1975; Brun et al., 1991), the Rio Grande Rift (Cordell, 1978; Mack and Seager, 1995), the Baikal Rift (Sherman, 1978; Hutchinson et al., 1992), the East African Rift System (EARS) (Morley, 1988; Ebinger, 1989a,b; Ebinger et al., 1989; Morley et al., 1990; Nelson et al., 1992), East Greenland (Larsen, 1988; Peacock et al., 2000b), the British Isles (Peacock and Sanderson, 1991; Huggins et al., 1995; Peacock, 2003), the Aegean Sea (Gawthorpe and Hurst, 1993), the Suez Rift

* Corresponding author. Tel.: +39-06-54888043; fax: +39-06-54888201
E-mail address: acocella@uniroma3.it (V. Acocella).

0191-8141/$ - see front matter © 2005 Elsevier Ltd. All rights reserved.
doi:10.1016/j.jsg.2004.11.006

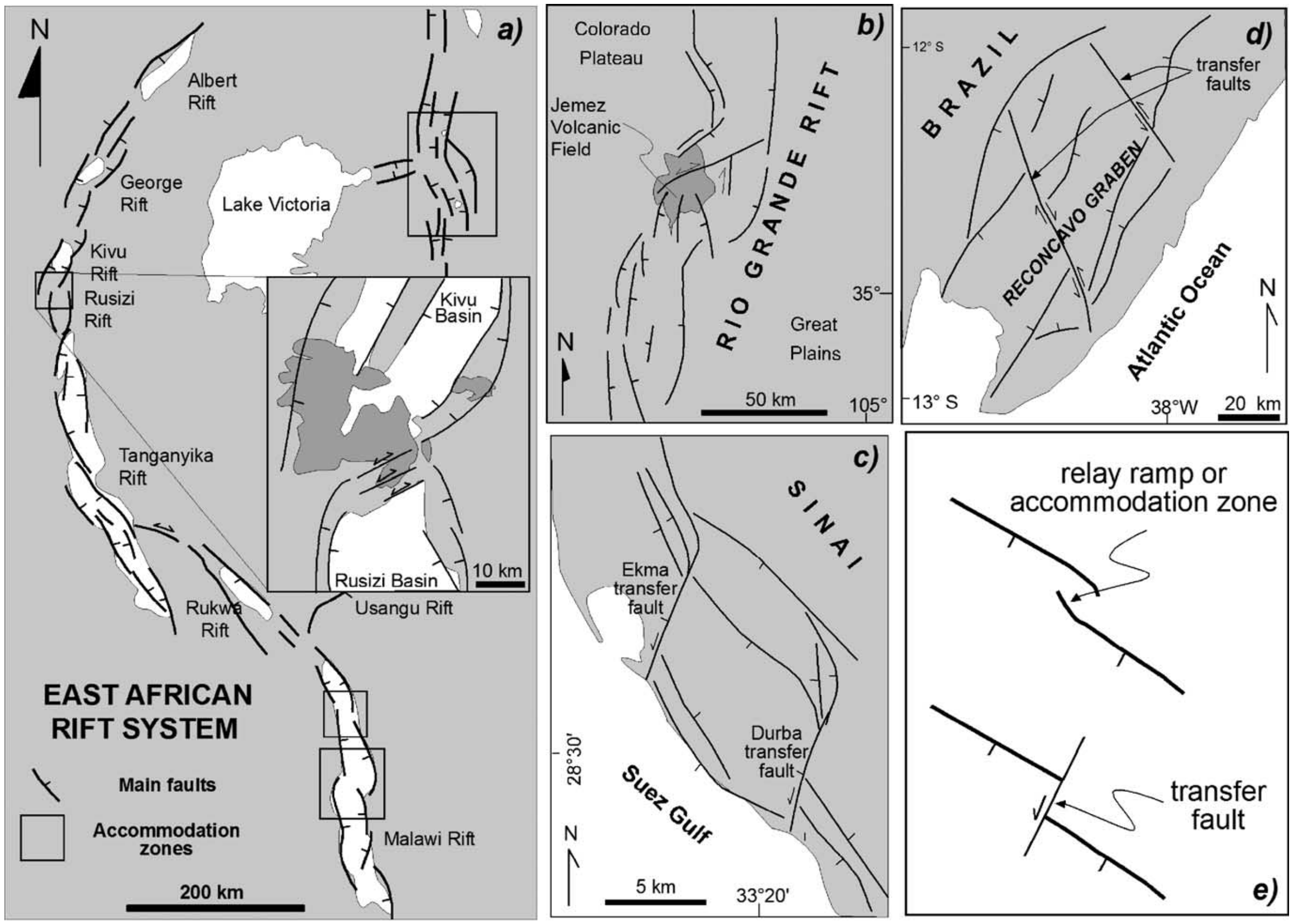

Fig. 1. Types of interaction between extensional structures at various rift zones: relay ramps in the East African Rift System (a) (after Ebinger, 1989b) and the Rio Grande graben (b) (after Aldrich, 1986); transfer faults in the Suez Rift (c) (after McClay and Khalil, 1998) and the Atlantic margin of Brazil (d) (after Milani and Davison, 1988); (e) schematic view of relay ramps and transfer faults in extensional domains.

(Moustafa, 1996), the Basin and Range (Anders and Schlische, 1994; Ferrill et al., 1999), the oceanic ridge of Iceland (Acocella et al., 2000) and the Gulf of Thailand (Kornsawan and Morley, 2002). In most of these cases, the relay ramps appear to control the shape or continuity of the rift and therefore they are considered significant at the rift scale (km to 10^3 km). Also, the geometric and kinematic features of relay ramps can be consistent over scales from m to 10^5 m (Acocella et al., 2000).

Transfer faults were first recognized and described in the Viking Graben, North Sea (Gibbs, 1984). Since then, various authors have reported the occurrence of transfer faults at various extensional settings, such as the Atlantic margin of Brazil (Milani and Davison, 1988), the Atlantic margin of Newark (Schlische, 1992), the Basin and Range (Duenbendorfer and Black, 1992; Martin et al., 1993), the Atlantic margin of Galicia (Boillot et al., 1995), the Atlantic margin of Namibia (Clemson et al., 1997), the Atlantic margin of Norway (Dorè et al., 1997; Tsikalas et al., 2001), the Suez Rift (McClay and Khalil, 1998), the Atlantic margin of W Africa (Watts and Stewart, 1998) and the Tyrrhenian (Acocella et al., 1999a) and Japanese (van der Werff, 2000) back-arc margins. In most of the cases, the transfer faults appear to be relevant at the rift scale (km to 10^2 km).

Therefore, while relay ramps are widespread in various extensional settings, transfer faults are usually observed within passive margins, wide rifts and back-arc basins, and are essentially lacking within continental narrow rifts (EARS, Rio Grande Rift, Rhine Graben and Baikal Rift). Also, within readily accessible oceanic extensional domains, such as Iceland, transfer faults are lacking and the dominant type of interaction are relay ramps (Acocella et al., 2000).

To investigate whether the selective occurrence of relay ramps and transfer zones is controlled by the differential extension along the rift, we have performed analogue experiments using sand (brittle crust analogue) and silicone (ductile crust analogue). The experiments simulate crustal blocks undergoing differential extension and show that transfer faults, relevant at the rift scale, can form only with a percentage of differential extension $\Delta e > 21 \pm 3\%$. Below this threshold, relay ramps, relevant at the rift scale, occur. This value roughly corresponds in nature to the threshold of

Table 1
Model and nature ratios applicable to the present study

Parameter	Model value	Nature value	Model/nature ratio
Length	0.01 m	10^4 m	$L^* \sim 10^{-6}$
Density	1.2–1.4 kg/m^3	2.4–2.8 kg/m^3	$\rho^* \sim 0.5$
Gravity	9.8 m/s^2	9.8 m/s^2	$g^* \sim 1$
Stress ($\sigma = \rho g L$)			$\sigma^* \sim 5 \times 10^{-7}$
Viscosity ($\mu = \sigma/\varepsilon$)	10^4–10^5 Pa s	10^{20}–10^{21} Pa s	$\mu^* \sim 10^{-16}$
Strain rate	5×10^{-6} s^{-1}	10^{-15} s^{-1}	$\varepsilon^* \sim 5 \times 10^9$
Time ($t = 1/\varepsilon$)			$t^* \sim 2 \times 10^{-10}$

extension between narrow continental rifts and oceanic ridges, where extension is lower and relay ramps are dominant, and wide rifts, passive margins and back-arc basins, where transfer faults are often more numerous.

2. Experimental procedure

2.1. Scaling and materials

Analogue experiments were constructed to simulate the interaction between adjacent crustal blocks experiencing different extension rates. Scaled models should be geometrically, kinematically and dynamically similar to natural examples (Ramberg, 1981, and references therein). In the experiments, the length ratio L between model and nature is $L^* = 10^{-6}$ (1 cm in our experiments corresponds to 10 km in nature), the density ratio between rocks and common experimental materials is $\rho^* \sim 0.5$ and the gravity ratio between model and nature is $g^* = 1$. The corresponding stress ratio between model and nature is $\sigma^* = \rho^* g^* z^* \sim 5 \times 10^{-7}$ (Table 1). Cohesion c has the dimensions of stress; assuming a Mohr–Coulomb criterion and natural cohesion $c \sim 10^7$ Pa, a material with $c \sim 5$ Pa is required to simulate the brittle crust: for this purpose, dry quartz sand, with $c \sim 0$ Pa, is used; the dry sand has a density ~ 1400 kg/m^3.

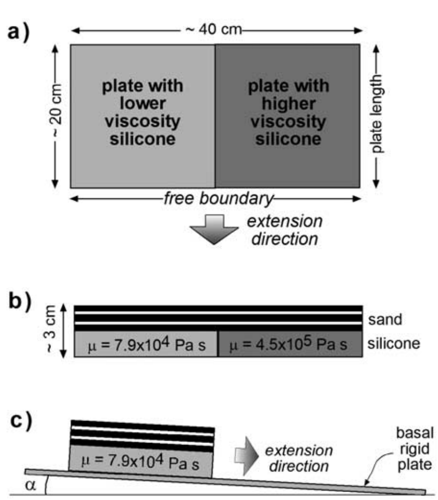

Fig. 2. Sketch of the experimental apparatus. (a) Map view; (b) frontal section view; (c) lateral section view.

Silicone putty with Newtonian behaviour has been used at the base of the sand-pack to simulate the plastically deforming crust. In order to reproduce different amounts of extension across the model, we use two adjacent layers of silicone, with different viscosities of 7.9×10^4 Pa s and 4.5×10^5 Pa s (Fig. 2b); the silicone has a density ~ 1310 kg/m^3.

The following relation applies to Newtonian ductile materials (Benes and Davy, 1996):

$$\sigma_1^* - \sigma_3^* = \mu^* \varepsilon^* \quad (1)$$

where μ^* and ε^* are the viscosity and the strain rate ratios between model and nature, respectively. Where $\sigma_1^* - \sigma_3^* \sim 5 \times 10^{-7}$, the μ^* and ε^* ratios have to be scaled accordingly (Table 1). Considering the viscosities of silicone and the mean viscosity of the lower crust (10^{20}–10^{21} Pa s; Ranalli, 1995), $\mu^* \sim 10^{-16}$ and, as a result (from Eq. (1)), $\varepsilon^* \sim 5 \times 10^9$. For a mean extensional strain rate $\varepsilon_n \sim 10^{-15}$ s^{-1}, commonly found in nature, to have $\varepsilon^* \sim 5 \times 10^9$, requires a strain rate $\varepsilon_m \sim 5 \times 10^{-6}$ s^{-1} in the experiments. As $\varepsilon^* = 1/t^*$, 1 s in our experiments corresponds to 2×10^{10} s (~ 634 years) in nature (Table 1).

2.2. Set-up

The experimental set-up is characterized by a 1–2-cm-thick sand layer, a 1–2-cm-thick silicone layer and a basal plate (Fig. 2). In all the experiments, the silicone layer consists of two adjacent silicone portions with different viscosity (Fig. 2a). The silicone layer is confined on three sides and has a free boundary along the fourth side.

Extension within the model is obtained by means of a moderate tilt (4–6°) of the basal plate towards the free boundary (Fig. 2c). The tilt angle has been chosen in order to maintain a consistence between the mean extension rates of the model and nature (Table 1). Such a tilt develops in fact a tangential (parallel to the dip of the tilted plate) component of the gravity force. The gravity force at the base of an experiment characterized by 1.5 cm of sand and 1.5 cm of silicone is:

$$\sigma = (\rho g z)_{\text{sand}} + (\rho g z)_{\text{silicone}} = 398.37\ \text{N}$$

For a basal tilt of 4°, the tangential stress at the base of the experiment is:

Table 2
Main imposed and observed features in the experiments. T_b = sand thickness; T_d = silicone thickness; L = length of model; W = width of model; μ_1 = viscosity of silicone in one plate; μ_2 = viscosity of silicone in the other plate; α = angle of tilting of the basal rigid plate; Δe = percentage of differential extension defining the experimental threshold between relay ramps and transfer faults

Experiment	T_b (cm)	T_d (cm)	L (cm)	W (cm)	μ_1 (Pa s)	μ_2 (Pa s)	α (°)	Δe
TIR 2	1	2	18	28	4.5×10^5	7.9×10^4	4	21
TIR 3	1	2	20	40	4.5×10^5	7.9×10^4	6	18
TIR 4	1.5	1.5	20	40	4.5×10^5	2.7×10^5	4	>10
TIR 5	1.5	1.5	25	40	4.5×10^5	7.9×10^4	4	23
TIR 6	1	2	20	50	4.5×10^5	7.9×10^4	4	20
TIR 7	1.5	2	20	40	4.5×10^5	7.9×10^4	4	24

$$\sigma_t = 398.37\cos4° = 27.8\ \mathrm{N}$$

This value represents the tangential component of the gravity force responsible for the flow of silicone along the slope at the beginning of the experiment (Fig. 2c).

The flow of silicone induces the thinning and extension of the overlying sand pack. As the silicone has different viscosities, it undergoes different flow velocities and therefore stretching. Since the amount of extension within the sand is proportional to the amount of stretching of the underlying silicone, this set-up simulates the interaction of adjacent blocks of upper crust with differential extension.

At the end of each experiment, sand was added and levelled onto the surface of the model, to preserve topography. The model was then saturated with water and cut. Six experiments were performed in order to test: the role of the ratio between the thickness of the brittle and ductile materials in the deformation pattern; the silicone viscosity contrast; the slope angle; the lateral dimensions of the models (Table 2).

This apparatus permits us to examine the interaction between structures undergoing differential extension without the control of a rigid basal velocity discontinuity, as commonly used in previous experiments of interacting extensional structures (Courtillot et al., 1974; Elmohandes, 1981; Serra and Nelson, 1988; Naylor et al., 1994; Mauduit and Dauteuil, 1996; Acocella et al., 1999b). The lack of a velocity discontinuity has the important advantage of avoiding the related modifications of the deformation pattern at surface.

2.3. Limits and assumptions of the experiments

These experiments study the effect of differential extension within a brittle crust; to achieve this, two silicone putties with different viscosities are used. The use of silicone with different viscosity does not necessarily correspond to the simulation of different types of ductile crust and therefore does not have a specific counterpart in nature. Silicone viscosity is thus varied to simulate a differential extension, not to simulate different types of ductile crust.

The tangential component of the gravity force σ_t responsible for the flow of silicone is not constant during the experiment. As the sand and silicone layers thin, σ_t decreases: σ_t at the end of the experiment can be estimated at 50% of the initial σ_t. This process is responsible for a decrease in the stretching rate with time, resulting in significant deformation of the model at the earlier stages and moderate deformation at later stages.

Variable extension rates are also found in natural extensional settings and, to a first approximation, assuming a variable extension rate should not limit the applicability of the experiments. Despite the variable extension rate, the total duration (~5 h) and extension (up to ~70%) of the experiments correspond to a realistic duration of rifting (~1.1×10^7 years) and amount of stretching in nature.

The experiments do not take into account any control of pre-existing brittle structures on the development of the interactions, even though these may play an important role. The purpose of the experiments is in fact the study of the type of interaction due to differential extension in the simplest conditions.

Finally, the types of interaction on which this work is focused are those characterizing the continuity and shape of the rift zones; therefore, only those interacting structures that appear relevant at the rift scale, both in nature and the experiments, are considered.

3. Experimental results

The evolution of the experiments is here summarized by model TIR 7 (T_b = 1.5 cm; T_d = 2 cm, where T_b and T_d are the sand and the silicone thickness, respectively), with silicone viscosities of 7.9×10^4 (left plate in Fig. 3a) and 4.5×10^5 Pa s (right plate in Fig. 3a). At $t=0'$ (minutes) the experiment is undeformed (Fig. 3a).

The tilt of the rigid base induces the flowing of silicone and extension in the two plates. At $t=60'$ several depressions form. The plate with more viscous silicone has four regularly spaced depressions bordered by normal faults, whereas the plate with less viscous silicone has six regularly spaced wider depressions bordered by normal faults (Fig. 3b). The lateral termination of these graben-like features along the contact between the adjacent plates is marked by relay ramps or accommodation zones. These consist of a broad deformed area, delimited by normal

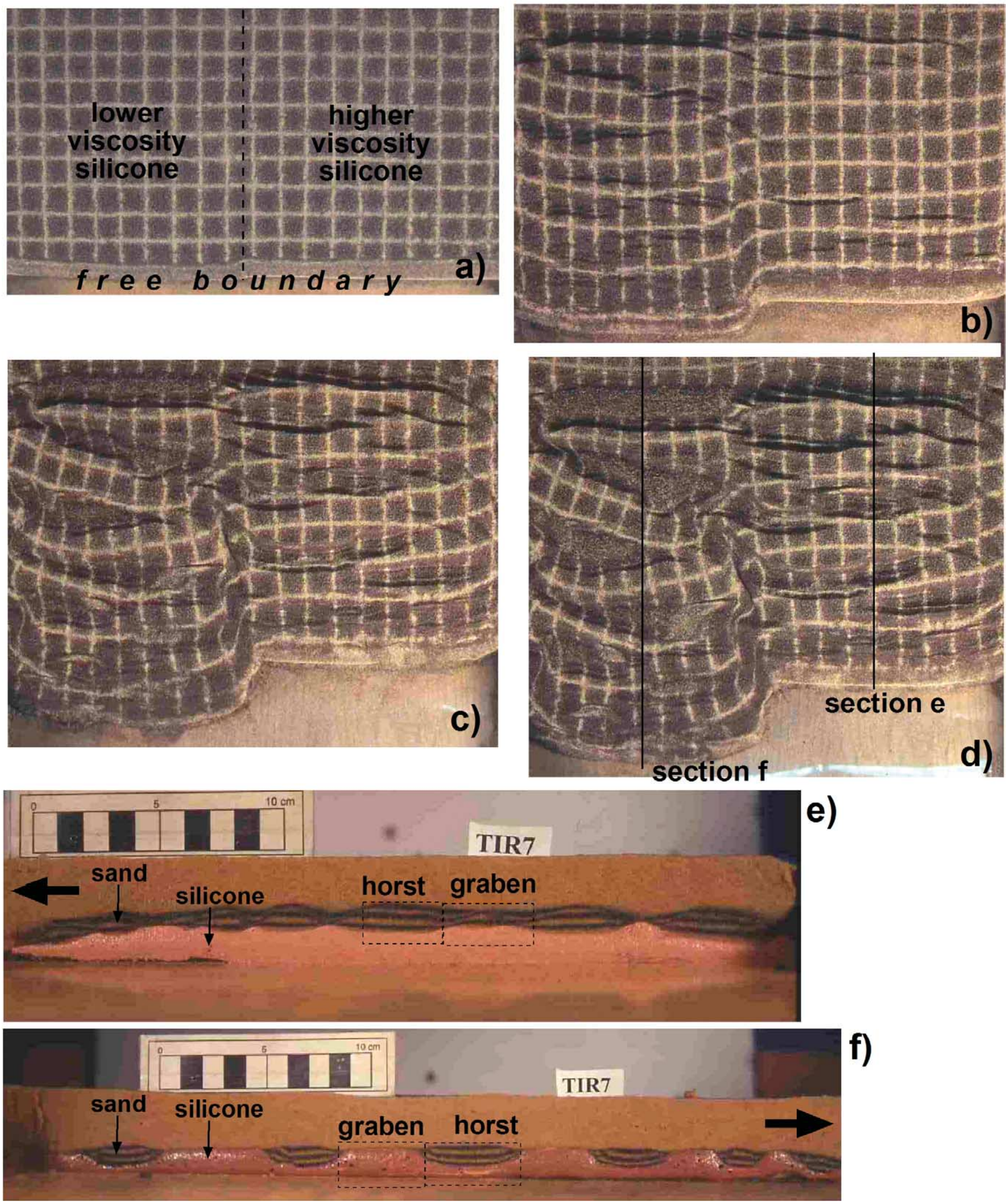

Fig. 3. Evolution of experiment TIR 7. Map views of: (a) undeformed stage; (b) experiment at $t=60'$; (c) experiment at $180'$; (d) experiment at $300'$. Enlarged section views along: (e) the plate with higher viscosity silicone; (f) the plate with lower viscosity silicone. Arrows in sections indicate the direction of extension; dashed rectangles show examples of horst and graben.

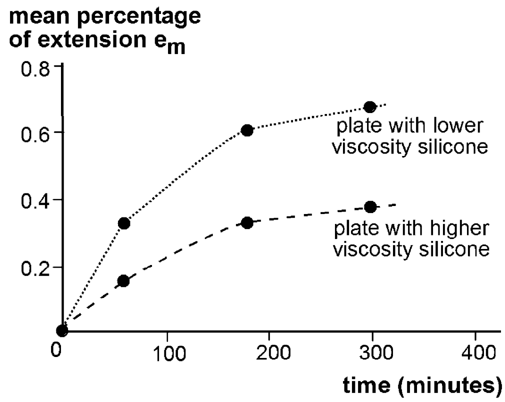

Fig. 4. Time variation of the mean percentage of extension for each plate.

faults, slightly oblique to the extension direction and displaying arcuate shapes.

At $t=180'$ the depressions have become wider and deeper (Fig. 3c). The interaction between the normal faults bordering these grabens now occurs with different modalities. Far from the free boundary, the interaction still occurs through relay ramps (Fig. 3c). Near the free boundary, the normal faults bordering the grabens are interrupted by a set of left-lateral faults subparallel to the extension direction (Fig. 3c). Therefore, the interaction between extensional structures here occurs by means of transfer faults.

At $t=300'$ the experiment does not show significant differences compared with the previous stage, even though the depressions are more accentuated and the strike-slip faults better developed (Fig. 3d).

The section view of the more viscous plate at the end of experiment is shown in Fig. 3e. Its thinning has been achieved through the development of a set of grabens and horst-like structures. The areas of maximum thinning in the brittle part correspond to the areas of rise of the underlying silicone putty.

The section view of the less viscous plate at the end of experiment is shown in Fig. 3f. The horst–graben configuration is here more pronounced, with local elision of the brittle overburden and rise of the silicone. The more severe thinning of this plate is related to the lower viscosity of the silicone.

The mean percentages of extension measured for each plate during the experiment are given by:

$$e_m = (L_m - L_i)/L_i$$

where L_i is the initial length of the plate and L_m is the incremental length of the plate after a given time interval. These percentages represent average values for each plate: at $60'$ (15 and 32%), $180'$ (32 and 60%) and $300'$ (37 and 67%) they show an overall decay in the amount of extension with time (Fig. 4).

The displacement vectors derived from the extension of

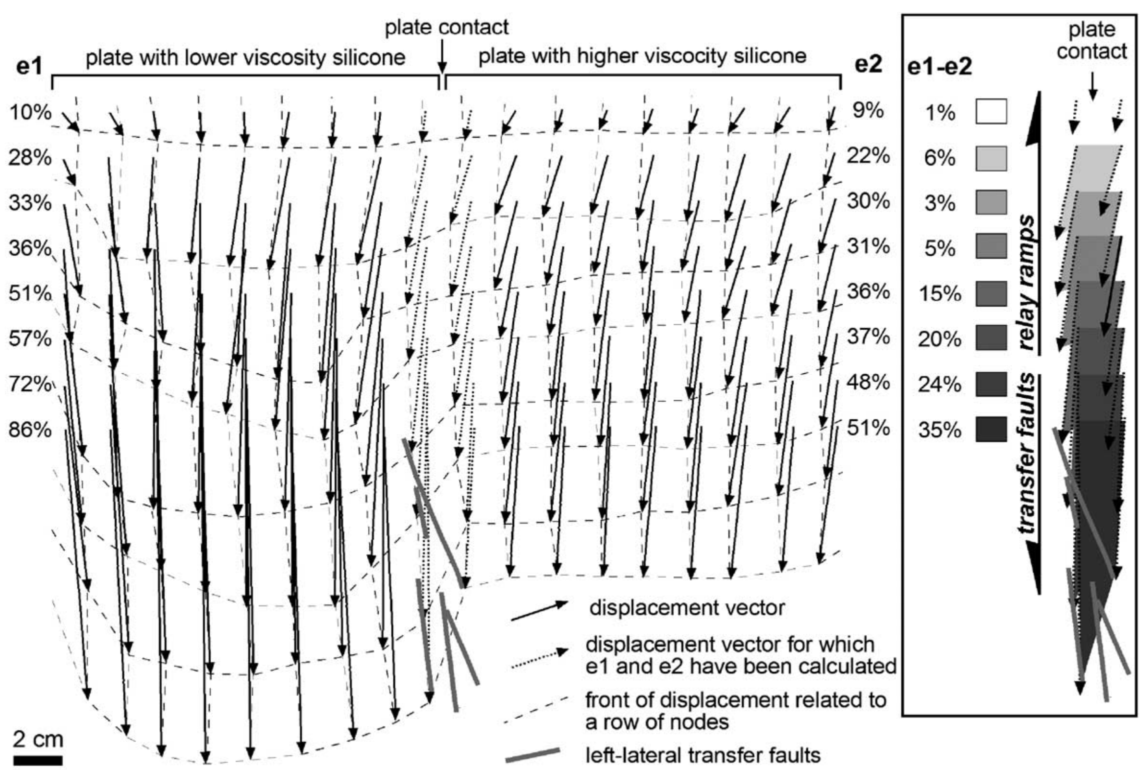

Fig. 5. Vectors of displacement of the nodes of the reference grid of experiment TIR 7 at the final stage of deformation ($t=300'$). The initial position of the nodes coincides with the origin of the arrows. e_1 and e_2 are the percentages of extension related to each couple of nodes (origin of the dotted arrows) at the two sides of the plates contact. The difference (e_1-e_2) between the percentages of extension for each couple of nodes at the sides of the contact gives the percentage of differential extension Δe. The inset highlights the variations of Δe (also represented as shades of grey) along the plate contact.

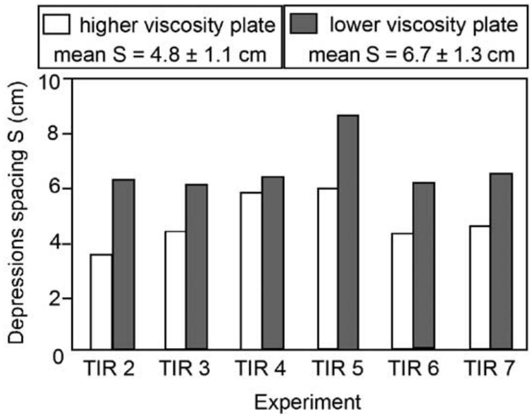

Fig. 6. Diagram showing the mean spacing of the depressions on the two plates for each experiment. The insets above report the mean spacing relative to all the experiments.

the reference grid at $t = 300'$ are shown in Fig. 5. In general, the vectors are longer on the low-viscosity plate and increase towards the free boundary. This implies that the differential extension at the contact between the two plates increases towards the free boundary as well.

Fig. 5 also shows the percentages of extension (e_1 and e_2) related to each couple of nodes (origin of the dotted arrows) at the border between the plate contact; these percentages are given, for each node, by:

$$e = (L_f - L_i)/L_i$$

where L_i is the initial length of the model and L_f is the incremental length of the node plus the initial length of the model L_i. The difference $(e_1 - e_2)$ between the percentages of extension for each couple of nodes at the sides of the contact gives the local percentage of differential extension Δe (inset in Fig. 5).

The shades of grey in Fig. 5 show that the presence of transfer faults (grey lines) connecting the two extending plates is limited to differential extension $\Delta e > 24\%$; below this threshold, the extending plates are connected by relay ramps. The differential extension of 24% represents therefore, in this experiment, the threshold between two types of interaction between extensional structures, characterized by relay ramps and transfer faults.

The remaining experiments, with the exception of TIR 4, showed an overall deformation pattern similar to TIR 7, despite their different model attributes (Table 2). The similar deformation pattern was produced during the development of relay ramps far from the free boundary and transfer faults near to the boundary. The values of differential extension associated with the presence of transfer faults are similar to TIR 7, giving a mean threshold of $21 \pm 3\%$ (Table 2). These data show that the presence of transfer faults in all the experiments is restricted, at any time during the evolution of an experiment, to a mean differential extension $> 21\%$; at lower values, relay ramps occur.

The depressions in both plates in all the experiments are regularly spaced. Their mean spacing, related to each plate and experiment, is shown in Fig. 6. The depressions on the lower viscosity plate have a slightly larger mean spacing ($S = 6.7$) with regard to those on the higher viscosity plate ($S = 4.8$).

The experimental transfer faults are usually arranged in subparallel segments. Their evolution is shown through different stages of experiment TIR 3 (Fig. 7); transfer faults usually grow in length through the linkage of en-échelon segments. Their propagation is mainly away from the free

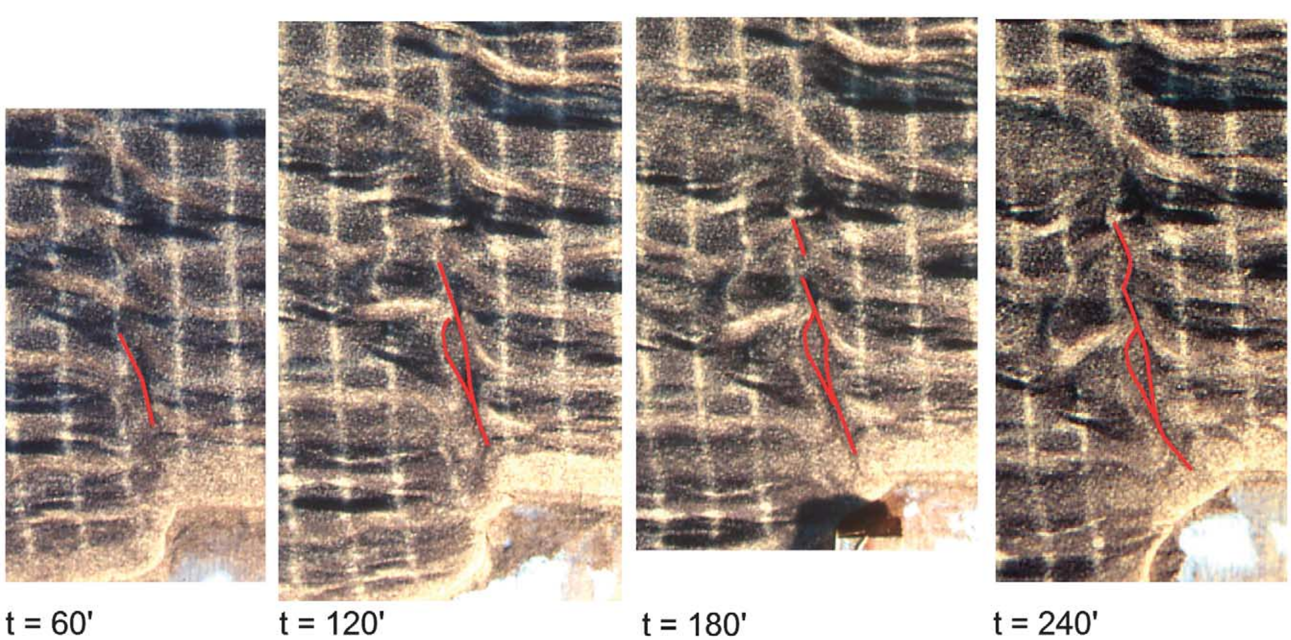

Fig. 7. Evolution of a transfer fault in experiment TIR 3.

Table 3
Estimates of β (and related references) for rift zones on Earth, Venus and Mars. The references describing the type of interaction (r.r. = relay ramps, t.f. = transfer faults) are given in the introduction

Rift type	Reference	Stretching β	Interaction type
Narrow rifts			
Rio Grande	(Golombek et al., 1983)	1.08	r.r.
Rhine graben	(Illies, 1979; Villemin et al., 1986)	1.13 ± 0.03	r.r.
East African Rift System	(Ebinger, 1989a; Prodehl et al., 1997)	1.15	r.r.
Baikal	(Agar and Klitgord, 1995)	1.16	r.r.
Oceanic ridges			
Iceland	(Forslund and Gudmundsson, 1991; Dauteuil et al., 2001)	< 1.06	r.r.
Extra-terrestrial narrow rifts			
Valles Marineris (Mars)	(Mege and Masson, 1996)	1.06	r.r.
Beta Regio (Venus)	(Foster and Nimmo, 1996)	1.1 ± 0.1	r.r.
Wide rifts			
Mojave Desert	(Martin et al., 1993)	1.5	t.f. + r.r.
Basin and Range	(Wernicke, 1985)	> 1.5	t.f. + r.r.
North Sea	(Latin and White, 1990)	2.5	t.f. + r.r.
Passive margins			
Brazil	(Milani and Davison, 1988)	1.39	t.f. + r.r.
Newark	(Schlische, 1992)	1.45	t.f. + r.r.
Suez	(Angelier, 1985)	1.45	t.f. + r.r.
NE Atlantic	(Tsikalas et al., 2001)	2.2	t.f. + r.r.
Galicia	(Boillot et al., 1995)	> 2.75	t.f. + r.r.
W Africa	(Watts and Stewart, 1998)	> 3	t.f. + r.r.
Back-arc basins			
Tyrrhenian margin	(Faccenna et al., 1997)	> 1.45	t.f. + r.r.
Japanese margin	(Jolivet et al., 1994)	1.8	t.f. + r.r.

boundary, because the percentage of differential extension is greatest at the free boundary and increases with time at all points along the transfer zone.

TIR 4 was the only experiment where transfer faults did not develop and was characterized by a lower viscosity contrast between the two silicone layers (viscosities of 1.7×10^5 and 4.5×10^5 Pa s). As a consequence, their maximum differential extension was ~10% and, consistently with the above results, the interaction between extensional structures in the two plates was characterized only by relay ramps.

4. Discussion and conclusions

4.1. Interpretation of the experiments

The tilt of the basal plate induces the downward flow of the silicone, causing extension of the model. At the very beginning, the low amount of extension within a restricted area is responsible for a deformation pattern interpretable as similar to the one of narrow rifts. At later stages, the higher amount of extension within a wider area is responsible for a deformation pattern more similar to the one of wide rifts. The rate of extension shows an overall decrease with time (Fig. 4), consistently with the decrease of σ_t.

The different viscosities of silicone at the base of the models are responsible for the differential extension. The experiments are all consistent with a differential extension associated with graben-like structures; these are, on the less viscous plate, more numerous, wider and deeper. The grabens show moderate variations in their spacing (Fig. 6), controlled by the interplay between the variations in T_b, T_d and the viscosity of silicone. In particular, the spacing S between instabilities responsible for the initiation of stretching of competent materials with thickness T_b follows the relationship $S\sim4T_b$ (Ricard and Froidevaux, 1986). Also, the instabilities developed during extension lead to the thinning of the sand overburden and the consequent rise of silicone; the lower the viscosity and the higher the thickness of silicone, the easier it will rise (Brun, 1999). A higher amount of risen silicone results in the higher spacing of the depressions (Fig. 3f). Similar processes have been used to study different modalities of continental extension, assuming therefore a general significance (Brun, 1999, and references therein).

Since the silicone nearer to the free boundary moves further (Fig. 5), the differential extension Δe ($\Delta e = e_1 - e_2$)

increases towards the free boundary. As a result, two types of interaction develop due to the gradient of differential extension.

The type of interaction is a function of the percentage of differential extension between the two plates Δe. When $\Delta e < 21 \pm 3\%$, the interaction occurs through relay ramps or accommodation zones. Their evolution can be characterized by the following stages (Fig. 3): (a) lateral propagation of the faults; (b) linkage with the adjacent structure. Their overall evolution is therefore similar to that of the natural prototypes (e.g. Acocella et al., 2000, and references therein). When $\Delta e > 21 \pm 3\%$, the interaction occurs through transfer faults. The experiments display the growth of the transfer faults, due to the linkage of smaller en-échelon strike-slip segments (Fig. 7): because of their geometries and kinematics, these segments can be interpreted as Reidel systems R of the growing transfer fault.

The experiments suggest that relay ramps, usually characterized by a minor component of strike-slip, accommodate minor differential displacements between two adjacent extensional structures. Conversely, larger differential displacements can be only accommodated by predominant strike-slip systems parallel to the extension direction, such as transfer faults.

The very moderate scatter ($\pm 3\%$) of the experimental threshold suggests that geometric parameters (such as the ratio between the thickness of the brittle and ductile materials, the slope angle and the lateral dimensions of the models) do not significantly affect the overall modalities of deformation, the types of interaction and their threshold value. The 3% scatter is moderate also when compared with the variations in the spacing (approximately $\pm 20\%$; Fig. 6) of the depressions; this suggests that the development of the type of interaction is independent from the overall configuration (frequency or spacing) of the extensional structures. Moreover, the fact that the two types of interaction occur above the contact between the silicone layers confirms that the latter does not influence the type of deformation, depending entirely on the amount of differential extension.

4.2. Comparison with nature

A qualitative comparison between our experiments and nature shows that the analogue faults share close geometric and kinematic similarities with those observed in extensional settings Also, the overall deformation pattern is consistent with the ones observed at various rifts, such as the Basin and Range, the Aegean Sea or the Tyrrhenian area (Duenbendorfer and Black, 1992; Gawthorpe and Hurst, 1993; Martin et al., 1993; Acocella and Funiciello, 2004).

A quantitative comparison is limited by the insufficient knowledge of the percentages of differential extension between crustal portions in rift zones. This constitutes a significant limitation for the complete and rigorous application of the results to nature. In fact, what is usually known about a rift zone is its overall stretching factor β, where $e = (\beta - 1) \times 100$, rather than the differential extension between its portions.

The β estimates for various extensional settings and the related references are shown in Table 3; the references describing the type of interaction observed in each setting are listed in the introduction. Table 3 shows that the narrow rifts (EARS, Baikal Rift, Rhine Graben, Rio Grande Rift) are characterized by a stretching factor $\beta < 1.16$. In contrast, the wide rifts (Basin and Range, North Sea), back-arc basins (Tyrrhenian Sea, Japan Sea) and passive margins at various stages of evolution (Suez Rift, Atlantic margins of Brazil, W Africa, Newark, Galicia and Norway) are characterized by higher stretching factors, where $\beta > 1.39$.

These data suggest that at narrow rifts, characterized by a limited amount of stretching ($\beta < 1.16$), significant (relevant at the rift scale) transfer faults cannot usually form. In fact, as the experiments suggest that transfer faults occur for $\Delta e > 21\%$, a differential extension within the narrow rift requires, to form transfer faults, stretching values higher ($\beta > 1.21$) than those measured. As a result, at narrow rifts relay ramps are the commonly observed type of interaction between extensional structures (Illies, 1975; Cordell, 1978; Sherman, 1978; Morley, 1988; Ebinger, 1989a,b; Brun et al., 1991; Hutchinson et al., 1992; Mack and Seager, 1995) and significant transfer faults are lacking. The formation of transfer faults for $\Delta e < 21\%$ may indeed be possible, provided there is a presence of pre-existing structures, subparallel to the extension direction, along the boundary between extending crustal portions. In this case, their reactivation may form transfer faults. Evidence for reactivated transfer faults is found in the Apennines of central Italy, where pre-existing NE–SW structures are reactivated as transtensive under NW–SE regional extension, with $\Delta e < 21\%$ (Acocella and Funiciello, 2004). Also, transfer-like features in the EARS have been interpreted as due to the reactivation of pre-existing structures (Rosendahl, 1987).

Conversely, on wide rifts, back-arc basins and passive margins, where $\beta > 1.39$, the kinematic conditions required to develop transfer faults can be fully met. Where the percentage of differential extension remains at $\Delta e < 21\%$, relay ramps continue to form. Nevertheless, because of the larger extension involved, a non-uniform extension may locally allow $\Delta e > 21\%$, developing transfer faults; this could be more easily achieved in those settings characterized by the highest β (Table 3). As a result, both transfer faults (Gibbs, 1984; Milani and Davison, 1988; Schlische, 1992; Martin et al., 1993; Boillot et al., 1995; Clemson et al., 1997; Dorè et al., 1997; McClay and Khalil, 1998; Watts and Stewart, 1998; Acocella et al., 1999a; van der Werff, 2000; Tsikalas et al., 2001) and relay ramps (Larsen, 1988; Gawthorpe and Hurst, 1993; Anders and Schlische, 1994; Moustafa, 1996; Ferrill et al., 1999; Peacock et al., 2000b) are commonly observed as types of interaction between extensional structures where $\beta > 1.21$ (Table 3).

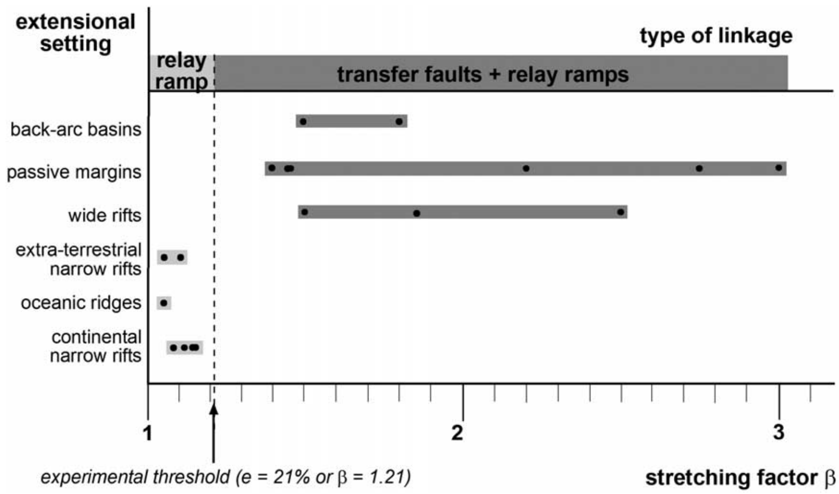

Fig. 8. Types of interaction within rift zones on Earth, Venus and Mars as a function of the stretching factor β. Relay ramps are widespread and independent from β. Transfer faults are observed only where $\beta > 1.39$. The experimental threshold ($e = 21\%$ or $\beta = 1.21$) coincides with the separation between domains where relay ramps (continental narrow rifts, oceanic ridges and extra-terrestrial narrow rifts) and relay ramps and transfer faults (wide rifts, passive margins, back-arc basins) have been observed.

These considerations show an overall consistency between the experimental data and the continental extensional domains. As far as oceanic extensional domains are concerned, the best-studied ridge is possibly the Icelandic Ridge. Calculations of its crustal dilation suggest a maximum $\beta = 1.06$ (Forslund and Gudmundsson, 1991; Dauteuil et al., 2001) and therefore transfer faults should be inhibited. This is in agreement with the fact that transfer faults are not observed within the ridge of Iceland and that the dominant type of interaction are relay ramps (Acocella et al., 2000).

Rift zones are also found on other terrestrial planets, characterized by a rigid lithosphere. Among these, the best-known cases are Beta Regio (Venus) and Valles Marineris (Mars), both consisting of narrow rifts, with overall deformation patterns similar to the rifts on Earth (Frey, 1979; Foster and Nimmo, 1996; Anderson et al., 2001). These planets exhibit gravity forces and crustal thickness that are different to those on Earth. Even though the performed experiments have not been specifically built to take into account these variations, it is nevertheless interesting to consider that these rift zones are likely associated with a maximum $\beta = 1.1$ (Foster and Nimmo, 1996; Mege and Masson, 1996) and lack of transfer fault-like structures. Therefore, their overall geometry and kinematics may be consistent with the experimental results and the Earth analogues.

The comparison between the experimental data and the considered continental and oceanic rifts on Earth and selected examples form terrestrial planets suggests a consistency in the type of interaction between extensional structures within rift zones (Fig. 8). This consistency consists of the widespread presence of relay ramps within rift zones characterized by moderate stretching factors ($\beta <$ 1.16) and both of transfer faults and relay ramps within rift zones characterized by higher stretching factors ($\beta > 1.39$). In the latter case, it is proposed that the amount of differential stretching Δe between adjacent extensional structures will locally determine the occurrence of transfer faults ($\Delta e > 21\%$) or relay ramps ($\Delta e < 21\%$).

Acknowledgements

C. Faccenna is acknowledged for helping in the set-up of the experiments and a critical read of the manuscript. N. D'Agostino kindly provided Fig. 5. Suggestions from J.P. Brun, A. Nicol and A.E. Clifton helped to significantly improve the work. Work partly financed with GNV (Campi Flegrei Project) Funds.

References

Acocella, V., Funiciello, R., 2004. Transverse structures and volcanic activity along the Tyrrhenian margin of central Italy. Proceedings of the 32nd International Geological Congress, Florence, Italy, p. 106.

Acocella, V., Salvini, F., Funiciello, R., Faccenna, C., 1999a. The role of transfer structures on volcanic activity at Campi Flegrei (Southern Italy). Journal of Volcanology and Geothermal Research 91, 123–139.

Acocella, V., Faccenna, C., Funiciello, R., Rossetti, F., 1999b. Sand-box modelling of basement controlled transfer zones in extensional domains. Terra Nova 11, 149–156.

Acocella, V., Gudmundsson, A., Funiciello, R., 2000. Interaction and linkage of extensional fractures: examples from the rift zone of Iceland. Journal of Structural Geology 22, 1233–1246.

Agar, S.M., Klitgord, K.D., 1995. Rift flank segmentation and propagation: a neotectonic example from Lake Baikal. Journal of the Geological Society London 152, 849–860.

Aldrich, M.J., 1986. Tectonics of the Jemez Lineament in the Jemez Mountains and Rio Grande Rift. Journal of Geophysical Research 91, 1753–1762.

Anders, M.H., Schlische, R.W., 1994. Overlapping faults, intrabasin highs and the growth of normal faults. The Journal of Geology 102, 165–180.

Anderson, R.C., Dohm, J.M., Golombek, M.P., Haldemann, A.F.C., Franklin, B.J., Tanaka, K.L., Lias, J., Peer, B., 2001. Primary centers and secondary concentrations of tectonic activity through time in the western hemisphere of Mars. Journal of Geophysical Research 106, 20563–20585.

Angelier, J., 1985. Extension and rifting: the Zeit region, Gulf of Suez. Journal of Structural Geology 7, 605–612.

Benes, V., Davy, P., 1996. Modes of continental lithospheric extension: experimental verification of strain localization processes. Tectonophysics 254, 69–87.

Boillot, G., Beslier, M.O., Krawczyk, C.M., Rappin, D., Reston, T.J., 1995. The formation of passive margins: constraints from the crustal structure and segmentation of the deep Galicia margin, Spain, in: Scrutton, R.A., Stoker, M.S., Shimmield, G.B., Tudhope, A.W. (Eds.), The Tectonics, Sedimentation and Palaeoceanography of the North Atlantic Region Geological Society Special Publication, 90, pp. 71–91.

Brun, J.P., 1999. Narrow rifts versus wide rifts: inferences for the mechanics of rifting from laboratory experiments. Philosophical Transactions of the Royal Society London 257, 695–712.

Brun, J.P., Wenzel, F., Ecors-Dekorp Team, 1991. Crustal-scale structure of the southern Rhinegraben from ECORS-DEKORP seismic reflection data. Geology 19, 758–762.

Clemson, J., Cartwright, J., Booth, J., 1997. Structural segmentation and the influence of basement structure on the Namibian passive margin. Journal of the Geological Society London 154, 477–482.

Cordell, L., 1978. Regional geophysical setting of the Rio Grande Rift. Geological Society of America Bulletin 89, 1073–1090.

Courtillot, V., Tapponier, P., Varet, J., 1974. Surface features associated with transform faults: a comparison between observed examples and an experimental model. Tectonophysics 24, 317–329.

Dauteuil, O., Angelier, J., Bergerat, F., Verrier, S., Villemin, T., 2001. deformation partitioning inside a fissure swarm of the northern Icelandic rift. Journal of Structural Geology 23, 1359–1372.

Dawers, N.H., Anders, M.H., 1995. Displacement–length scaling and fault linkage. Journal of Structural Geology 17, 607–614.

Dorè, A.G., Lundin, E.R., Fichler, C., Olesen, O., 1997. Patterns of basement structure and reactivation along the NE Atlantic margin. Journal of the Geological Society, London 154, 85–92.

Duenbendorfer, E.M., Black, R.A., 1992. Kinematic role of transverse structures in continental extension: an example from the Las Vegas Valley shear zone, Nevada. Geology 20, 1107–1110.

Ebinger, C.J., 1989a. Tectonic development of the western branch of the East African Rift System. Geological Society of America Bulletin 101, 885–903.

Ebinger, C.J., 1989b. Geometric and kinematic development of border faults and accommodation zones, Kivu–Rusizi Rift, Africa. Tectonics 8, 117–133.

Ebinger, C.J., Deino, A.L., Drake, R.E., Tesha, A.L., 1989. Chronology of volcanism and rift basin propagation: Rungwe Volcanic Province, East Africa. Journal of Geophysical Research 94, 15785–15803.

Elmohandes, S.E., 1981. The central European graben system: rifting imitated by clay modelling. Tectonophysics 73, 69–78.

Faccenna, C., Mattei, M., Funiciello, R., Jolivet, L., 1997. Styles of back-arc extension in the central Mediterranean. Terra Nova 9, 126–130.

Ferrill, D.A., Stamatakos, J.A., Sims, D., 1999. Normal fault corrugation: implications for growth and seismicity of active normal faults. Journal of Structural Geology 21, 1027–1038.

Forslund, T., Gudmundsson, A., 1991. Crustal spreading due to dikes and faults in southwest Iceland. Journal of Structural Geology 13, 443–457.

Foster, A., Nimmo, F., 1996. Comparison between the rift systems of East Africa, Earth and Beta Regio, Venus. Earth and Planetary Science Letters 143, 183–195.

Frey, H., 1979. Martian Canyons and African Rifts: structural comparison and implications. Icarus 37, 142–155.

Gawthorpe, R.L., Hurst, J.M., 1993. Transfer zones in extensional basins: their structural style and influence on drainage development and stratigraphy. Journal of the Geological Society, London 150, 1132–1137.

Gibbs, A.D., 1984. Structural evolution of extensional basin margins. Journal of the Geological Society, London 141, 609–620.

Gibbs, A.D., 1990. Linked faults in basin formation. Journal of Structural Geology 12, 795–803.

Golombek, M.P., McGill, G.E., Brown, L., 1983. Tectonic and geologic evolution of the Espanola basin, Rio Grande rift: structure, rate of extension and relation to the state of stress in the Western United States. Tectonophysics 94, 483–507.

Huggins, P., Watterson, J., Walsh, J.J., Childs, C., 1995. Relay zone geometry and displacement transfer between normal faults recorded in coal-mine plans. Journal of Structural Geology 17, 1741–1755.

Hutchinson, D.R., Golmshtok, A.J., Zonenshain, L.P., Moore, T.C., Scholz, C.A., Klitgord, K.D., 1992. Depositional and tectonic framework of the rift basins of Lake Baikal from multichannel seismic data. Geology 20, 589–592.

Illies, J.H., 1975. Recent and paleo-intraplate tectonics in stable Europe and the Rhine graben Rift System. Tectonophysics 29, 251–264.

Illies, J.H., 1979. Holocene movements and state of stress in the Rhinegraben Rift System. Tectonophysics 52, 349–359.

Jolivet, L., Tamaki, K., Fournier, M., 1994. Japan Sea, opening history and mechanism: a synthesis. Journal of Geophysical Research 99, 22237–22259.

Kornsawan, A., Morley, C.K., 2002. The origin and evolution of complex transfer zones (graben shifts) in conjugate fault systems around the Funan Field, Pattani Basin, Gulf of Thailand. Journal of Structural Geology 24, 435–449.

Koukouvelas, I.K., Asimakopoulos, M., Doutsos, T.T., 1999. Fractal characteristics of active normal faults: an example of the eastern Gulf of Corinth, Greece. Tectonophysics 308, 263–274.

Larsen, P.H., 1988. Relay structures in a Lower Permian basement-involved extension system, Early Greenland. Journal of Structural Geology 10, 3–8.

Latin, D., White, N., 1990. Generating melt during lithospheric extension: pure shear vs. simple shear. Geology 18, 327–331.

Macdonald, K.C., Fox, P.J., 1983. Overlapping spreading centres: new accretion geometry on the East Pacific Rise. Nature 302, 55–58.

Mack, G.H., Seager, W.R., 1995. Transfer zones in the Southern Rio Grande Rift. Journal of the Geological Society, London 152, 551–560.

Martin, M.W., Glazner, A.F., Walker, J.D., Schermer, E.R., 1993. Evidence for right lateral transfer faulting accommodating en echelon Miocene extension Mojave Desert, California. Geology 21, 355–358.

Mauduit, T., Dauteuil, O., 1996. Small-scale models of oceanic transform zones. Journal of Geophysical Research 101, 20195–20209.

McClay, K., Khalil, S., 1998. Extensional hard linkages, eastern Gulf of Suez, Egypt. Geology 26, 563–566.

Mege, D., Masson, P., 1996. Amounts of crustal stretching in Valles Marineris, Mars. Planetary and Space Science 44, 749–761.

Milani, E.J., Davison, I., 1988. Basement control and transfer tectonics in the Reconcavo–Tucano–Jatoba rift, Northeast Brazil. Tectonophysics 154, 41–70.

Morley, C.K., 1988. Variable extension in Lake Tanganyika. Tectonics 7, 785–801.

Morley, C.K., Nelson, R.A., Patton, T.L., Munn, S.G., 1990. Transfer zones in the East African Rift System and their relevance to hydrocarbon exploration in rifts. American Association of Petroleum Geology 74, 1234–1253.

Moustafa, A.R., 1996. Internal structure and deformation of an accommodation zone in the northern part of the Suez rift. Journal of Structural Geology 18, 93–107.

Naylor, M.A., Larroque, J.M., Gauthier, B.D.M., 1994. Understanding extensional tectonics: insights from sand-box models, in: Roure, F., Ellouz, N., Shein, V.S., Skvortsov, I. (Eds.), Geodynamic Evolution of Sedimentary Basins, International Symposium, Moscow, pp. 69–83.

Nelson, R.A., Patton, T.L., Morley, C.K., 1992. Rift–segment interaction and its relation to hydrocarbon exploration in continental rift systems. American Association of Petroleum Geology Bulletin 76, 1153–1169.

Peacock, D.C.P., 2003. Scaling of transfer zones in the British Isles. Journal of Structural Geology 25, 1561–1567.

Peacock, D.C.P., Sanderson, D.J., 1991. Displacement, segment linkage and relay ramps in normal fault zones. Journal of Structural Geology 13, 721–733.

Peacock, D.C.P., Knipe, R.J., Sanderson, D.J., 2000a. Glossary of normal faults. Journal of Structural Geology 22, 291–305.

Peacock, D.C.P., Price, S.P., Whitham, A.G., Pickles, C.S., 2000b. The world's biggest relay ramp: Hold with Hope, NE Greenland. Journal of Structural Geology 22, 843–850.

Pollard, D.D., Aydin, A., 1988. Progress in understanding jointing over the past century. Geological Society of America Bulletin 100, 1181–1204.

Prodehl, C., Fuchs, K., Mechie, J., 1997. Seismic refraction studies of the Afro–Arabian rift system—a brief review. Tectonophysics 278, 1–13.

Ramberg, H., 1981. Gravity, Deformation and the Earth's Crust in Theory, Experiments and Geological Applications. Academic Press, London.

Ranalli, G., 1995. Rheology of the Earth. Chapman & Hall, London.

Ricard, Y., Froidevaux, C., 1986. Stretching instabilities and lithospheric boudinage. Journal of Geophysical Research 91, 8314–8324.

Rosendahl, B.R., 1987. Architecture of continental rifts with special reference to East Africa. Annual Review of Earth and Planetary Science 15, 445–503.

Schlische, R.W., 1992. Structural and stratigraphic development of the Newark extensional basin, eastern North America: evidence for the growth of the basin and its bounding structures. Geological Society of America Bulletin 104, 1246–1263.

Serra, S., Nelson, R.A., 1988. Clay modeling of rift asymmetry and associated structures. Tectonophysics 153, 307–312.

Sherman, S.I., 1978. Faults of the Baikal rift zone. Tectonophysics 45, 31–39.

Tsikalas, F., Faleide, J.I., Eldholm, O., 2001. Lateral variations in tectono-magmatic style along the Lofoten–Vesteralen volcanic margin off Norway. Marine and Petroleum Geology 18, 807–832.

Villemin, T., Alvarez, F., Angelier, J., 1986. The Rhine graben: extension, subsidence and shoulder uplift. Tectonophysics 128, 47–59.

Walsh, J.J., Watterson, J., 1991. Geometric and kinematic coherence and scale effects in normal fault systems, in: Roberts, A.M., Yelding, G., Freeman, B. (Eds.), The Geometry of Normal Faults Geological Society of London Special Publication, 56, pp. 193–206.

Watts, A.B., Stewart, J., 1998. Gravity anomalies and segmentation of the continental margin offshore West Africa. Earth and Planetary Science Letters 156, 239–252.

van der Werff, W., 2000. Backarc deformation along the eastern Japan Sea margin, offshore northern Honshu. Journal of Asian Earth Sciences 18, 71–95.

Wernicke, B., 1985. Uniform-sense normal simple shear of the continental lithosphere. Canadian Journal of Earth Sciences 22, 108–125.